Supporting Information

Harnessing Lewis Acidic Open Metal Sites of Metal-organic Frameworks: Foremost Route to Achieve Highly Selective Benzene Sorption over Cyclohexane

Soumya Mukherjee,[a] Biplab Manna,[a] Aamod V. Desai,[a] Yuefeng Yin,[b] Rajamani Krishna,[c] Ravichandar Babarao,*[d] and Sujit K. Ghosh*[a]

[a]Indian Institute of Science Education and Research (IISER), Dr. Homi Bhabha Road, Pashan, Pune-411008, India.

Fax: +91 20 2590 8186. E-mail: sghosh@iiserpune.ac.in

[b]Department of Materials Science and Engineering, Monash University, Clayton, Victoria 3800, Australia.

[c]Van ‘t Hoff Institute for Molecular Sciences, University of Amsterdam, Science Park 904, 1098 XH Amsterdam, The

Netherlands.

[d]Manufacturing, Commonwealth Scientific and Industrial Research Organization (CSIRO), Clayton, Victoria 3168, Australia. E-mail: Ravichandar.Babarao@csiro.au

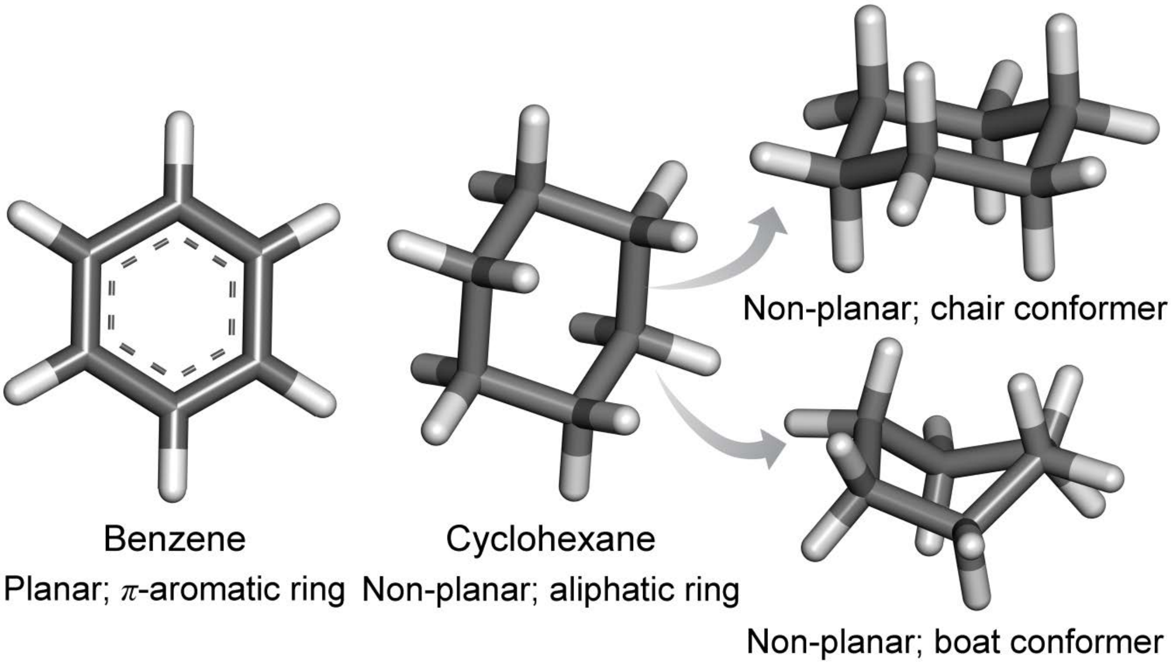

Figure S1: General conformations of planar aromatic π-ring Benzene (Bz) (left) and non-planar aliphatic congener Cyclohexane (Cy) (middle): chair (top right) and boat (bottom right) conformers.

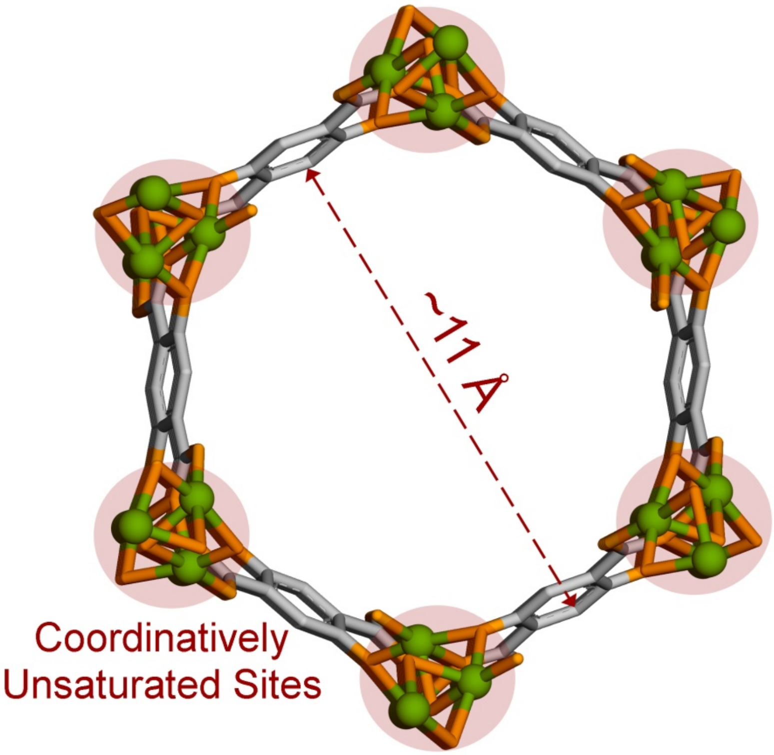

Figure S2: Orthographic view of a single pore along crystallographic *c*-axis; the pore being decorated with open metal sites or coordinatively unsaturated metal centres, with a window size ~ 11 Å.

Table S1. Physical Properties of C_6 adsorptive species.

Dimensions of Adsorptive molecules (Å)[S1] (each atom surrounded by a van der Waals sphere)						Boiling and Freezing Points		Conformers
Dimensional Closeness								
	x	***y***	**z**	**MIN-1**	**MIN-2**	**B.P.**	**F.P.**	**Type(s)**
Bz	6.628	7.337	3.277	3.277	6.628	353.3 K	278.7 K	Planar
Cy	7.168	6.580	4.982	4.982	6.580	353.9 K	279.6 K	Non-planar: Boat and Chair

MIN-1: Size of the adsorptive in the minimum dimension.

MIN-2: Second minimum dimension for molecular orientations that enable a molecule to enter the channel.

Table S2. Comparative analysis of the saturation uptake amounts recorded for the C_6-hydrocarbon pair Benzene and Cyclohexane in case of all the seven **M-MOF-74** compounds.

Compound	**Bz Saturation Uptake Amounts (12.5 KPa) (mmolg^{-1})**	**Cy Saturation Uptake Amounts (12.5 KPa) (mmolg^{-1})**
Mg-MOF-74	8.15	0.40
Mn-MOF-74	9.38	0.25
Fe-MOF-74	5.50	0.15
Co-MOF-74	5.57	0.23
Ni-MOF-74	9.19	0.09
Cu-MOF-74	7.55	0.13
Zn-MOF-74	6.76	0.17

Experimental Section:

Materials and measurements:

Unless otherwise noted, all the reagents and solvents were commercially available and used without further purification. Physical measurements:

Powder X-ray diffraction (PXRD) patterns were measured on Bruker D8 Advanced X-Ray diffractometer at room temperature using Cu-Kα radiation (λ= 1.5406 Å) with a scan speed of 0.5° min^{-1} and a step size of 0.01° in 2 *theta*. Thermogravimetric analysis was recorded on Perkin-Elmer STA 6000, TGA analyzer under N_2 atmosphere with heating rate of 10° C/min.

Low-Pressure Solvent Sorption Measurements

Low-pressure solvent (Bz and Cy) sorption measurements were performed using BelAqua (Bel Japan). As-synthesized **M-MOF-74** compounds (as prepared by the reported protocols)[9e, 12c,13] were exchanged thrice each day over a period of seven days with fresh batches of dry methanol, before heating each at 210 °C under vacuum to end up with guest-free, activated crystalline phases, suitable for sorption analysis.

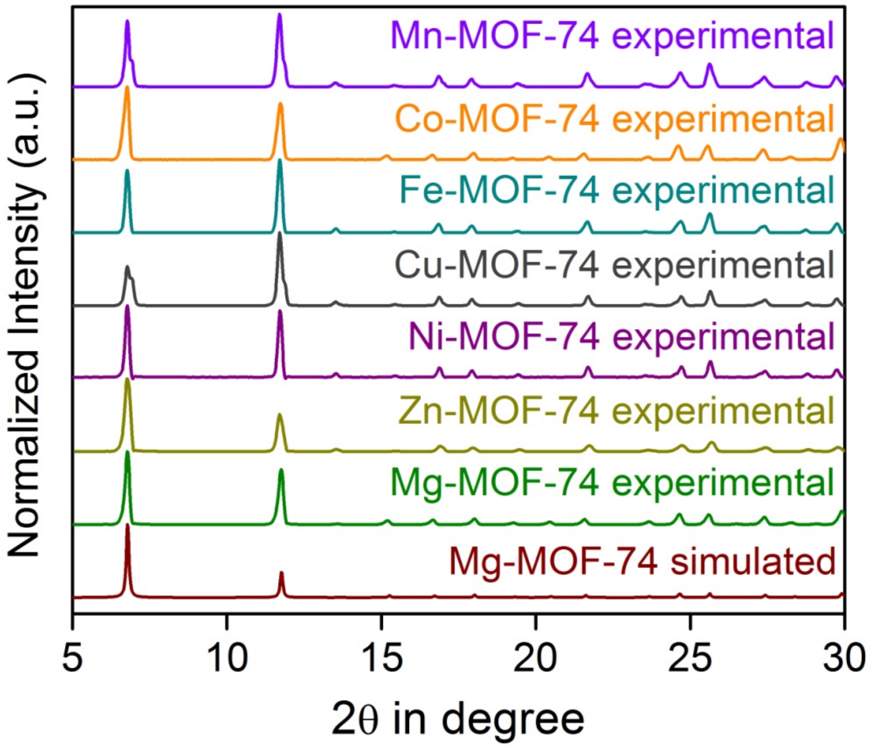

Figure S3: Similar experimental PXRD profiles for all the seven **M-MOF-74** analogous compounds, plotted relative to the simulated pattern of **Mg-MOF-74**.

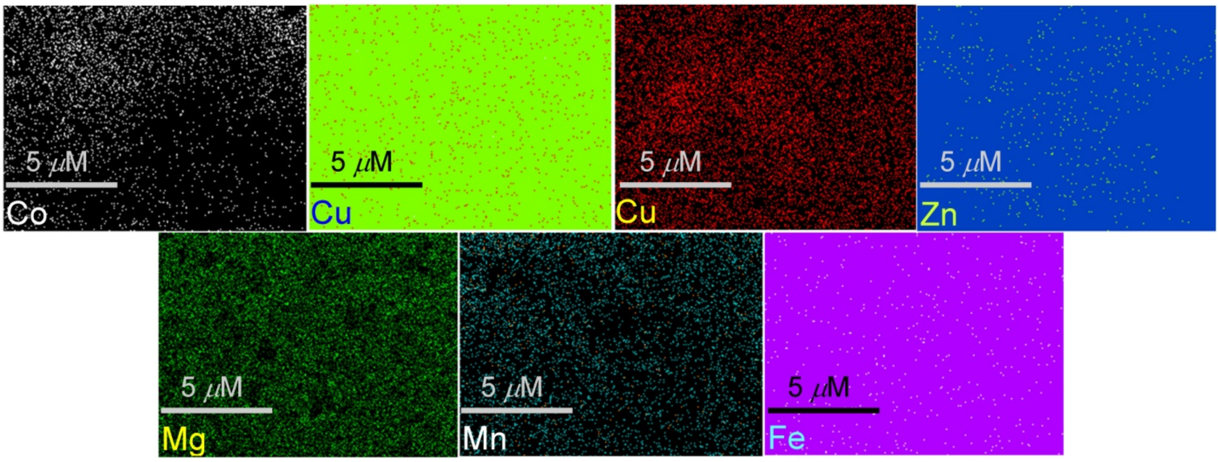

Figure S4: Elemental mapping (EDX) images of the different metals in cases of the seven **M-MOF-74** compounds.

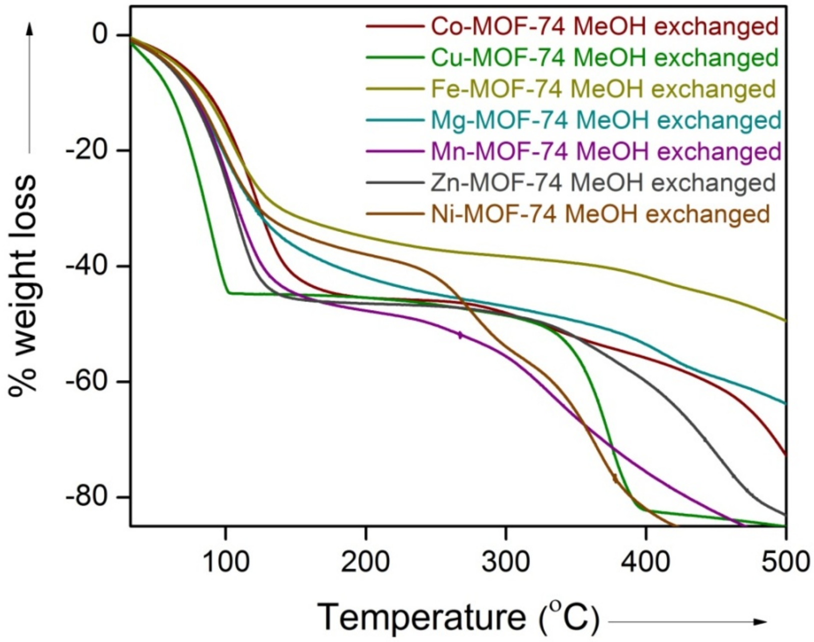

Figure S5: Thermogravimetric analysis profiles for the MeOH-exchanged phases of **M-MOF-74** compounds.

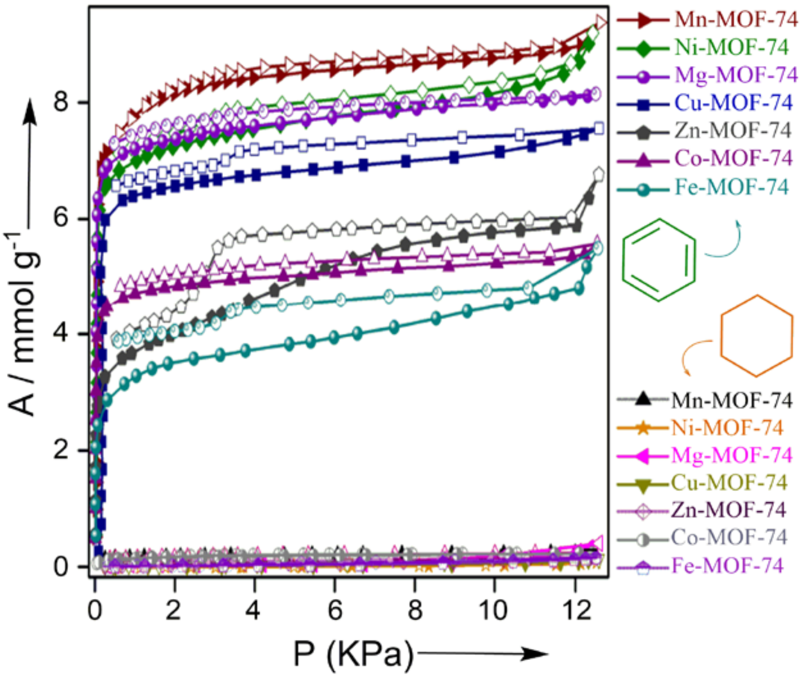

Figure S6: Single component solvent sorption isotherms (Bz and Cy) for the series of **M-MOF-74** (M= Mg, Mn, Fe, Co, Ni, Cu, Zn) compounds recorded at 298 K (in terms of mmol per g versus P in KPa). Filled and open markers denote adsorption and desorption, respectively.

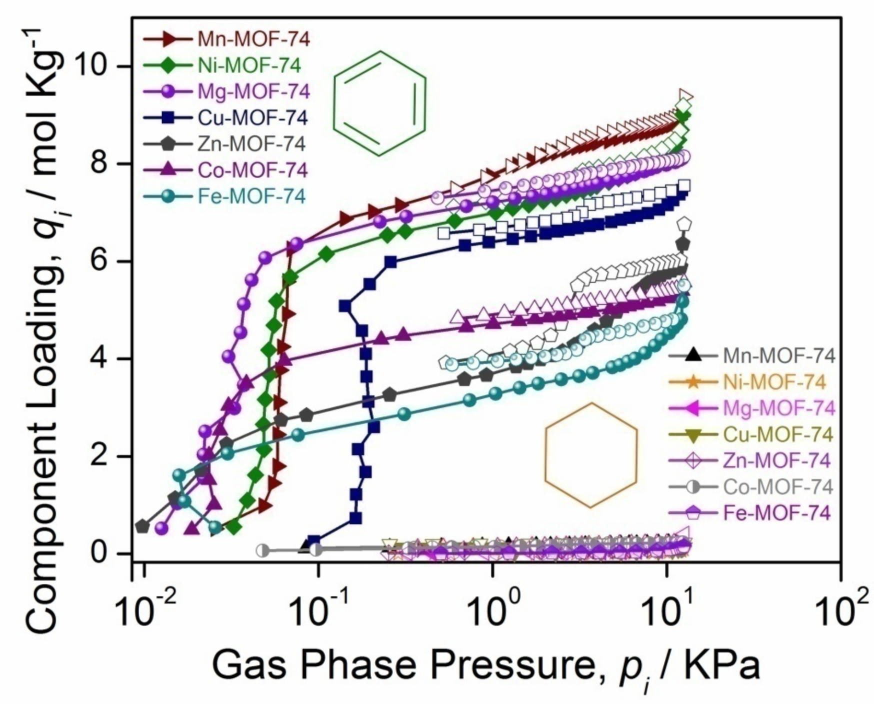

Figure S7: Comparison of unary benzene isotherms in **M-MOF-74** at 298 K.

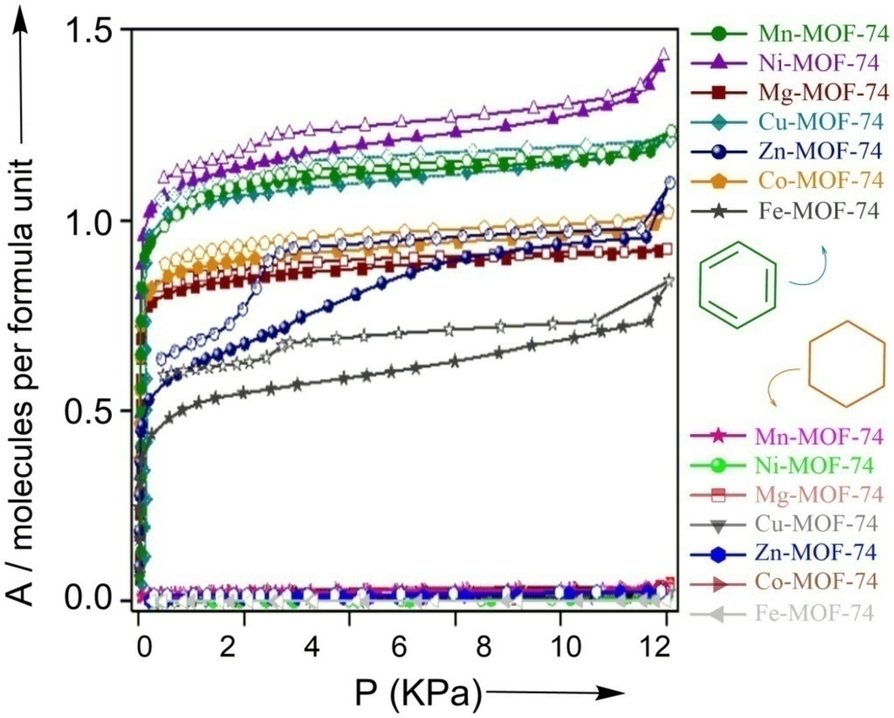

Figure S8: Single component solvent sorption isotherms (Bz and Cy) for the series of **M-MOF-74** (M= Mg, Mn, Fe, Co, Ni, Cu, Zn) compounds recorded at 298 K (in terms of molecules per formula unit versus P in KPa). Filled and open markers denote adsorption and desorption, respectively.

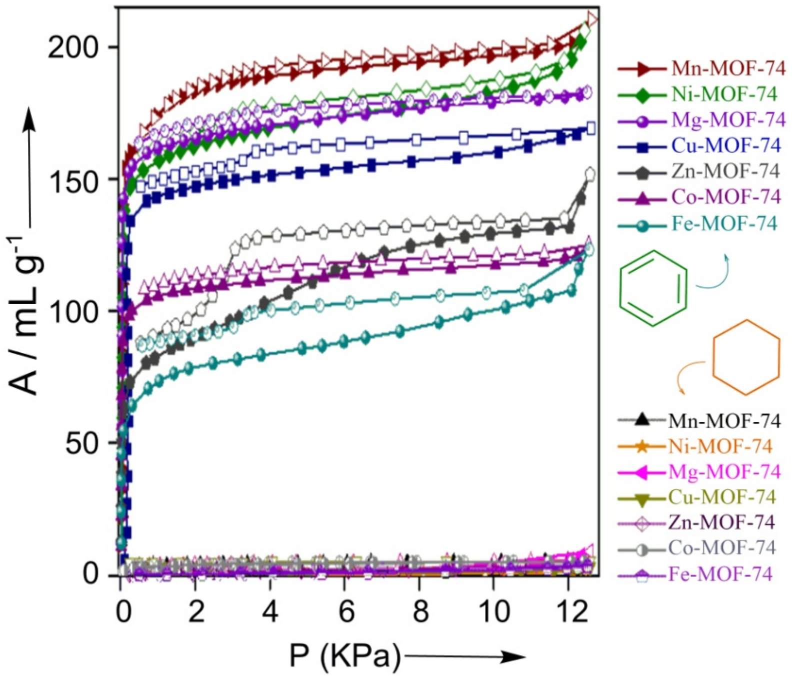

Figure S9: Single component solvent sorption isotherms (Bz and Cy) for the series of **M-MOF-74** (M= Mg, Mn, Fe, Co, Ni, Cu, Zn) compounds recorded at 298 K (in terms of mL per gram versus P in KPa). Filled and open markers denote adsorption and desorption, respectively.

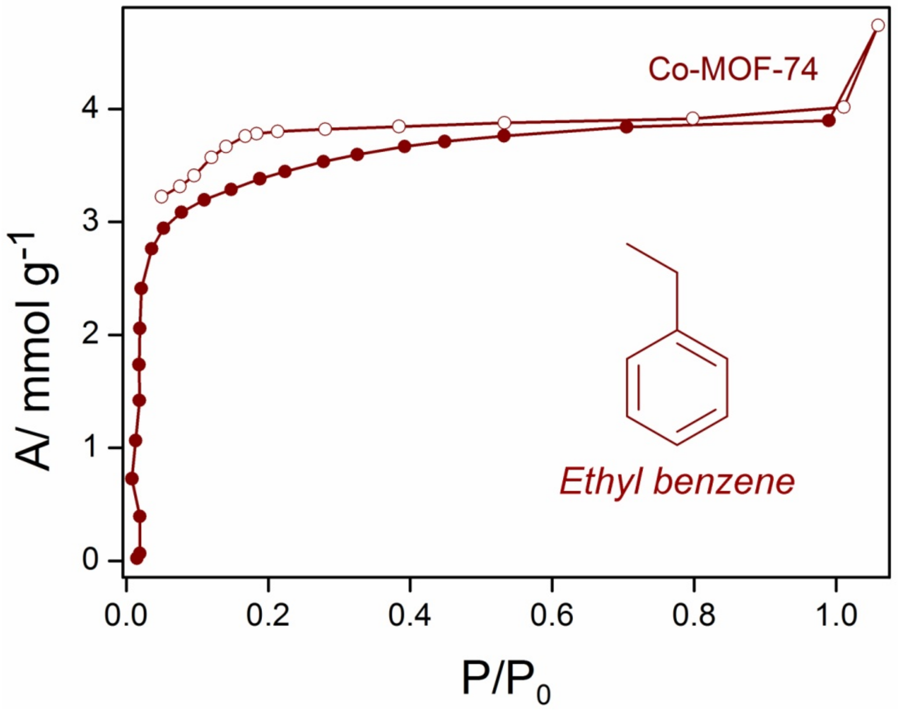

Figure S10: Single component ethyl benzene sorption isotherm for **Co-MOF-74** (one representative among the series of **M-MOF-74**), recorded at 298 K (in terms of mmol per gram versus P/P_0). Filled and open markers denote adsorption and desorption, respectively.

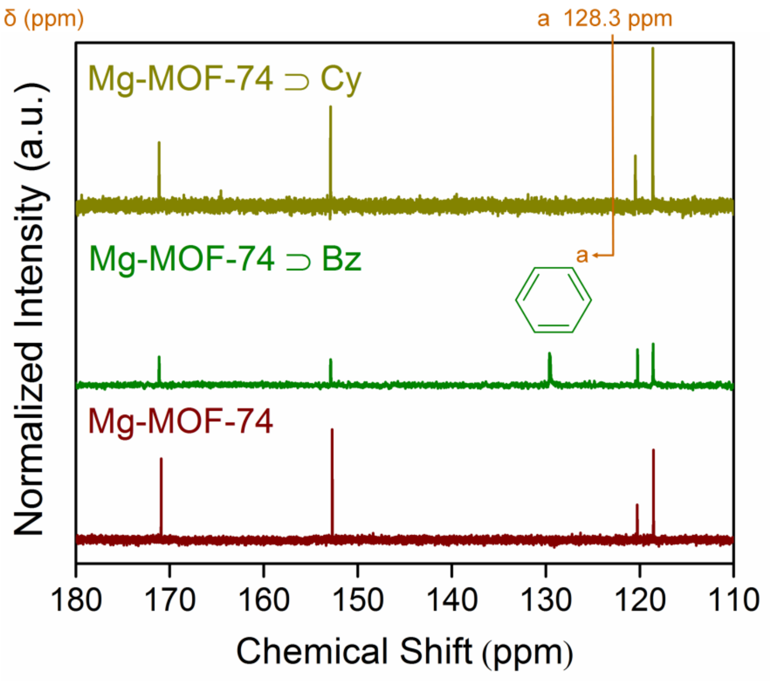

Figure S11: ^{13}C NMR spectra for Bz and Cy vapor-exposed phases of compound **Mg-MOF-74**, as compared to the desolvated phase itself.

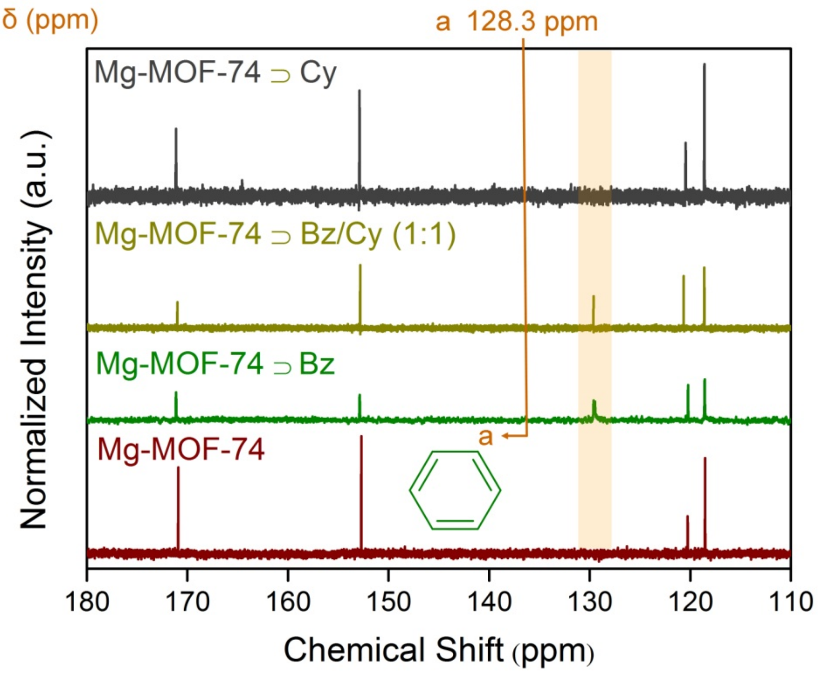

Figure S12: ^{13}C NMR spectra for 1:1 equimolar mixtures of Bz/Cy exposed phase of **Mg-MOF-74**, as compared to the Bz and Cy vapor-exposed phases of compound **Mg-MOF-74**, and the one for desolvated phase itself.

Simulation Methodology

NVT simulation:

The initial geometry of benzene molecule in **M-MOF-74** (M – Mg, Mn, Fe, Co, Cu, Zn and Ni) was estimated based on simulated annealing method using classical force field as implemented in sorption module in *Materials Studio*.[S2] The crystal structures for the **M-MOF-74** were taken from the literature.[S3-S5] The configurational-bias algorithm was used rather than the conventional *Metropolis* technique, which is prohibitively expensive in sampling the phase space of big molecules. In configurational-bias algorithm, a molecule is grown atom-by-atom biasing energetically favorable configurations while avoiding overlap with other atoms.[S6, S7] The simulation box contained super cell and the periodic boundary conditions were exerted in all three dimensions. In the simulated annealing method, the temperature is lowered in succession allowing the gas molecule to reach a desirable configuration based on different moves such as rotate, translate and re-position with preset probabilities of occurrence. This process of heating and cooling the system was repeated in several heating cycles to find the local minima. Forty heating cycles were performed where the maximum temperature and the final temperature were 10^5 K and 100 K, respectively. The NVT ensemble process consisted of 10^7 equilibration steps followed by 10^7 production steps, with the properties calculated from the latter steps. The LJ interactions were evaluated using a spherical cutoff of 12.5 Å and the Coulombic interactions were calculated using the Ewald summation with a precision of 10^{-5}. Five types of trial moves were randomly attempted in the MC simulation, namely, translation, rotation, twist, regrowth, and exchange including creation and deletion with equal probability.

The long-range Coulombic interactions are computed with a Ewald summation technique using point charges assigned to both the framework atoms and the guest molecules. The point charges assigned to the framework atoms are adopted from earlier work reported in the literature.[S8, S9] Dispersion interaction energies are computed from a Lennard-Jones potential form with parameters from the universal force field (UFF)[S10] for both the framework atom and guest molecule. The Lorentz− Berthelot mixing rule is used for the pairwise interaction parameters between two different atomic species.

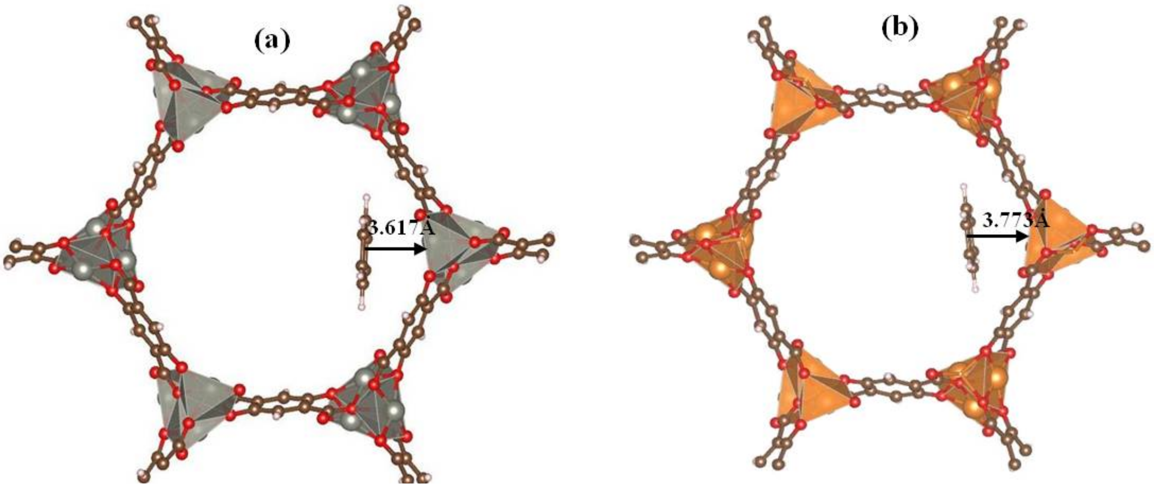

Figure S13. Location of benzene in (a) **Zn-MOF-74**, and (b) **Mg-MOF-74** identified from NVT simulated annealing method. For clarity the hexagonal cell is cleaved from the supercell to represent the location of guest molecule. The distance between the centriod of benzene and metal ion is shown in angstroms. Similarly for other **M-MOF-74** analogues, we obtained the lowest energy configuration of benzene using simulated annealing method.

Density Functional Theory (DFT) calculations

Static binding energies for benzene molecule at 0 K were calculated using the van der Waals density functional (vdW-DF) method.[S11] All calculations were performed using Vienna *ab initio* simulation package (VASP)[S12, S13] with a plane-wave energy cut-off of 860 eV and k-point sampling at the gamma-point. Hubbard U corrections are not included in the calculation. The interactions between core and valence electrons were described by the projector-augmented-wave (PAW) method[S14] and revPBE[S15] was used to parameterize the exchange-correlation functional. Recent studies revealed that the binding energy and the distance between benzene and transition metal surfaces obtained from vdW-DF and vDW-DF2 are more or less similar, but differ significantly from those of the opt-type van der Waals functionals.[S16] However, the different functional used in vdW-DF are not tested in this work as no experimental heat of adsorption is available to validate the methods.

The initial location of single benzene molecule in the periodic cell was obtained from the classical simulated annealing technique as described in the NVT simulation section. During relaxation, both the lattice vectors and the atomic positions are simultaneously optimized. The atomic positions and the lattice vectors are optimized until the residual forces are smaller than 0.01 eV/Å. Static binding energies (ΔE) at 0 K were calculated using the following expression;

$$\Delta E = E_{MOF+benzene} - E_{MOF} - E_{benzene}$$

where E_x refers, respectively, to the total energies of the MOF + benzene complex, the MOF alone, and benzene molecule.

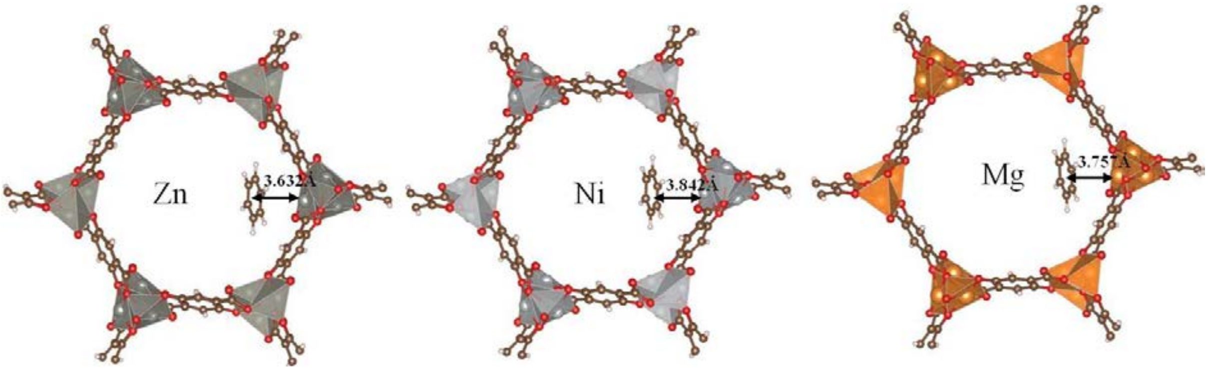

Figure S14. Optimized location of benzene based on van der Waals density functional in **M-MOF-74** analogues. The distance between the centre of the benzene molecule and the transition metals are shown in angstroms.

Table S3. Vdw-DF calculated adsorption energies (in kJ/mol) of a single benzene molecule in **M-MOF-74** analogues.

M-MOF-74	ΔE^a
Ni-MOF-74	-71.77
Mn-MOF-74	-68.09
Zn-MOF-74	-68.95
Mg-MOF-74	-67.57
Cu-MOF-74	-66.86
Co-MOF-74	-65.49
Fe-MOF-74	-65.31

[a] ΔE refers to the static 0 K adsorption energy.

Table S4. Three-site Langmuir-Freundlich parameters for adsorption of benzene in **M-MOF-74** at 298 K.

$$q = q_{A,sat}\frac{b_A p^{\nu_A}}{1+b_A p^{\nu_A}} + q_{B,sat}\frac{b_B p^{\nu_B}}{1+b_B p^{\nu_B}} + q_{C,sat}\frac{b_C p^{\nu_C}}{1+b_C p^{\nu_C}}$$

	Site A			**Site B**			**Site C**		
	$q_{\mathrm{A,sat}}$ mol kg^{-1}	b_{A} $\mathrm{Pa}^{-\nu_A}$	ν_A dimensionless	$q_{\mathrm{B,sat}}$ mol kg^{-1}	b_{B} $\mathrm{Pa}^{-\nu_B}$	ν_B dimensionless	$Q_{\mathrm{C,sat}}$ mol kg^{-1}	b_{C} $\mathrm{Pa}^{-\nu_C}$	ν_C dimensionless
Mn	1	0.00004	1	5.5	1E-25	14	3	0.005	1
Ni	0.5	0.00004	1	4.65	1.2E-25	15	3.2	0.005	1
Mg	0.4	0.00004	1	5.5	1.2E-25	18	2.3	0.005	1
Cu	0.4	0.00001	1	5.1	1E-33	14.5	2.2	0.001	1
Zn	2.3	0.00001	1	2.5	1E-07	6	2.5	0.001	1
Co	0.4	0.00004	1	3.5	1.2E-25	18	1.5	0.005	1
Fe	2.2	0.00001	1	2.3	1E-07	6	2	0.001	1

For a binary mixture the adsorption selectivity is defined as follows

$$S_{ads} = \frac{q_1/q_2}{p_1/p_2}$$

Table S5. Two-site Langmuir-Freundlich parameters for adsorption of cyclohexane in **M-MOF-74** at 298 K.

$$q = q_{A,sat} \frac{b_A p^{\nu_A}}{1 + b_A p^{\nu_A}} + q_{B,sat} \frac{b_B p^{\nu_B}}{1 + b_B p^{\nu_B}}$$

	Site A			**Site B**		
	$q_{\mathrm{A,sat}}$ mol kg^{-1}	b_{A} $\mathrm{Pa}^{-\nu_A}$	ν_A dimensionless	$q_{\mathrm{B,sat}}$ mol kg^{-1}	b_{B} $\mathrm{Pa}^{-\nu_B}$	ν_B dimensionless
Mn	0.19	0.01	1	0.3	2E-08	1.7
Ni	0.7	0.000001	1	0.2	1E-29	7
Mg	1	0.00001	1	1	1E-46	11
Cu	5	0.000001	1	1	1E-34	8
Zn	0.15	0.0002	1	0.1	0.00004	1
Co	0.14	0.01	1	0.1	0.0002	1
Fe	5	0.000001	1	1	1E-34	8

Notation

b_A	dual-Langmuir-Freundlich constant for species *i* at adsorption site A, $\mathrm{Pa}^{-\nu_i}$
b_B	dual-Langmuir-Freundlich constant for species *i* at adsorption site B, $\mathrm{Pa}^{-\nu_i}$
c_i	molar concentration of species *i* in fluid mixture, mol m^{-3}
c_{i0}	molar concentration of species *i* in fluid mixture at inlet to adsorber, mol m^{-3}
L	length of packed bed adsorber, m
n	number of species in the mixture, dimensionless
p_i	partial pressure of species *i* in mixture, Pa
p_t	total system pressure, Pa
q_i	component molar loading of species *i*, mol kg^{-1}
$q_{i,sat}$	molar loading of species *i* at saturation, mol kg^{-1}
q_t	total molar loading in mixture, mol kg^{-1}
$q_{sat,A}$	saturation loading of site A, mol kg^{-1}
$q_{sat,B}$	saturation loading of site B, mol kg^{-1}
t	time, s
T	absolute temperature, K
u	superficial gas velocity in packed bed, m s^{-1}
v	interstitial gas velocity in packed bed, m s^{-1}

Greek letters

ε	voidage of packed bed, dimensionless
ν	exponent in dual-Langmuir-Freundlich isotherm, dimensionless
θ_t	fractional occupancy within the pores, dimensionless
ρ	framework density, kg m^{-3}
τ	time, dimensionless

Subscripts

i	referring to component *i*
A	referring to site A
B	referring to site B
t	referring to total mixture

References:

S1. C. E. Webster, R. S. Drago, and M. C. Zerner, *J. Am. Chem. Soc.*1998, **120**, 5509-5516.

S2. *Materials Studio, 7.0 ed.;*, Accelrys, San Diego, 2012.

S3. W. Zhou, H. Wu, and T. Yildirim, *J. Am. Chem. Soc.* 2008, **130**, 15268-15269.

S4. R. Sanz, F. Martinez, G. Orcajo, L. Wojtas, and D. Briones, *Dalton Trans.* **2013**, *42*, 2392-2398.

S5. D. J. Xiao, E. D. Bloch, J. A. Mason, W. L. Queen, M. R. Hudson, N. Planas, J. Borycz, A. L. Dzubak, P. Verma, K. Lee, F. Bonino, V. Crocella, J. Yano, S. Bordiga, D. G. Truhlar, L. Gagliardi, C. M. Brown, and J. R. Long, *Nat. Chem.* 2014, **6**, 590-595.

S6. D. Frenkel, G. Mooij, and B. Smit, *J. Phys.: Condensed Matter* 1992, **4**, 3053-3076.

S7. J. I. Siepmann, and D. Frenkel, *Mol. Phys.* 1992, **75**, 59-70.

S8. J. Borycz, L.-C. Lin, E. D. Bloch, J. Kim, A. L. Dzubak, R. Maurice, D. Semrouni, K. Lee, B. Smit, and L. Gagliardi, *J. Phys. Chem. C* 2014, **118**, 12230-12240.

S9. T. Pham, K. A. Forrest, J. Eckert, and B. Space, *Cryst. Growth Des.* 2016, **16**, 867-874.

S10. A. K. Rappe, C. J. Casewit, K. S. Colwell, W. A. Goddard, and W. M. Skiff, *J. Am. Chem. Soc.* 1992, **114**, 10024-10035.

S11. A. Puzder, M. Dion, and D. C. Langreth, *J. Chem. Phys.* 2006, **124**.

S12. G. Kresse, and J. Hafner, *Phys. Rev. B* 1993, **48**, 13115-13118.

S13. G. Kresse, and J. Furthmuller, *Comput. Mater. Sci.* 1996, **6**, 15-50.

S14. G. Kresse, and D. Joubert, *Phys. Rev. B* 1999, **59**, 1758-1775.

S15. M. Dion, H. Rydberg, E. Schroder, D. C. Langreth, and B. I. Lundqvist, *Phys. Rev. Lett.* 2004, **92**.

S16. J. Klimes, D. R. Bowler, and A. Michaelides, *J. Phys.: Condens. Matter* 2010, **22**.